Dyes and Pigments 94 (2012) 469–474

Contents lists available at SciVerse ScienceDirect

Dyes and Pigments

journal homepage: www.elsevier.com/locate/dyepig

Novel D–A–π–A coumarin dyes containing low band-gap chromophores for dye-sensitised solar cells

Kang Deuk Seo [a], In Tack Choi [a], Young Geun Park [b], Sunwoo Kang [b], Jin Yong Lee [b], Hwan Kyu Kim [a,*]

[a] Department of Advanced Materials Chemistry and Center for Advanced Photovoltaic Materials, Korea University, Jochiwon, Chungnam 339-700, Republic of Korea
[b] Department of Chemistry, Sungkyunkwan University, Suwon 440-746, Republic of Korea

ARTICLE INFO

Article history:
Received 19 December 2011
Received in revised form
21 February 2012
Accepted 22 February 2012
Available online 3 March 2012

Keywords:
Coumarin
Metal-free organic dyes
π-bridge units
Dye-sensitised solar cell
Low band-gap chromophore
Benzothiadiazole

ABSTRACT

Coumarin dyes containing a low band-gap chromophore of benzothiadiazole, which comprises a coumarin moiety as the electron donor and a cyanoacrylic acid moiety as electron acceptor in D–A–π–A system, were developed to use in dye-sensitised solar cells (DSSCs). The introduction of the benzothiadiazole unit into the molecular framve distinctly narrowed the band-gap between the highest occupied molecular orbital (HOMO) and the lowest unoccupied molecular orbital (LUMO), so that the absorption peak was red-shifted. As a result, a solar cell based on the **HKK-CM4** sensitiser showed better photovoltaic performance with a J_{SC} of 14.3 mA cm^{-2}, a V_{OC} of 0.58 V, and an FF of 0.72, corresponding to an overall conversion efficiency η of 5.97% under standard AM 1.5 irradiation.

1. Introduction

Dye-sensitised solar cells (DSSCs) based on mesoporous nanocrystalline TiO_2 films have attracted significant attention due to their low cost and high sunlight-to-electric power-conversion efficiencies of 10–11% [1–4]. In these cells, the sensitiser is one of the key components for high power-conversion efficiency; the Ru(II) complex is the most efficient heterogeneous charge-transfer sensitiser and is widely used in nanocrystalline TiO_2-based DSSC [5–9]. However, the main drawback of the Ru(II) complex sensitiser is the cost of ruthenium metal, the requirement for careful synthesis, and tricky purification steps [10].

In recent years, interest in metal-free organic dyes as an alternative to noble metal complexes has increased due to their many advantages, such as the diversity of molecular structures, high molar extinction coefficients, simple synthesis, as well as low cost and environmental issues. Many organic dyes, based on the donor–(π-spacer)–acceptor (D–π–A) system, exhibiting relatively high DSSC performance, have so far been designed and developed. They include coumarin dyes [11,12], triarylamine dyes [13–16], hemicyanine dyes [17,18], thiophene-based dyes [19], indoline dyes [20–26], porphyrin dyes [27–31], and phthalocyanine [32] dyes. Although remarkable progress has been made in the development of organic dyes as sensitisers for DSSCs, optimising their chemical structures is required for further improvements in performance. Among the metal-free organic dyes studied in DSSCs, coumarin-based dyes coupled to TiO_2 are promising sensitisers because of their good photoresponse in the visible region, good long-term stability under one sun-soaking [12,33], and appropriate lowest unoccupied molecular orbital (LUMO) levels matching the conduction band of TiO_2.

Tian et al. have reported a series of donor–acceptor–π–bridge–acceptor (D–A–π–A) structural organic dyes incorporating benzotiadiazole into the triphenylamine framework, resulting in red-shift in absorption and weakening the deprotonation effect on TiO_2 film, which is beneficial for light-harvesting [34]. Here, we report benzotiadiazole-substituted coumarin derivatives for the use in DSSCs, in which an electron-deficient benzotiadiazole unit is connected to a donor group in D–A–π–A chromophores with two following reasons: (i) the use of a π –extended benzothiadiazole derivative bridging unit between the coumarin donor and the cyanoacrylic acid anchoring group leads to more red shift of absorption and emission bands; (ii) the introduction of electron-rich 3,4-ethylenedioxythiophene (EDOT) unit is achieved to be

* Corresponding author. Tel.: +82 418601493; fax: +82 418675396.
E-mail address: hkk777@korea.ac.kr (H.K. Kim).

0143-7208/$ – see front matter © 2012 Elsevier Ltd. All rights reserved.
doi:10.1016/j.dyepig.2012.02.015

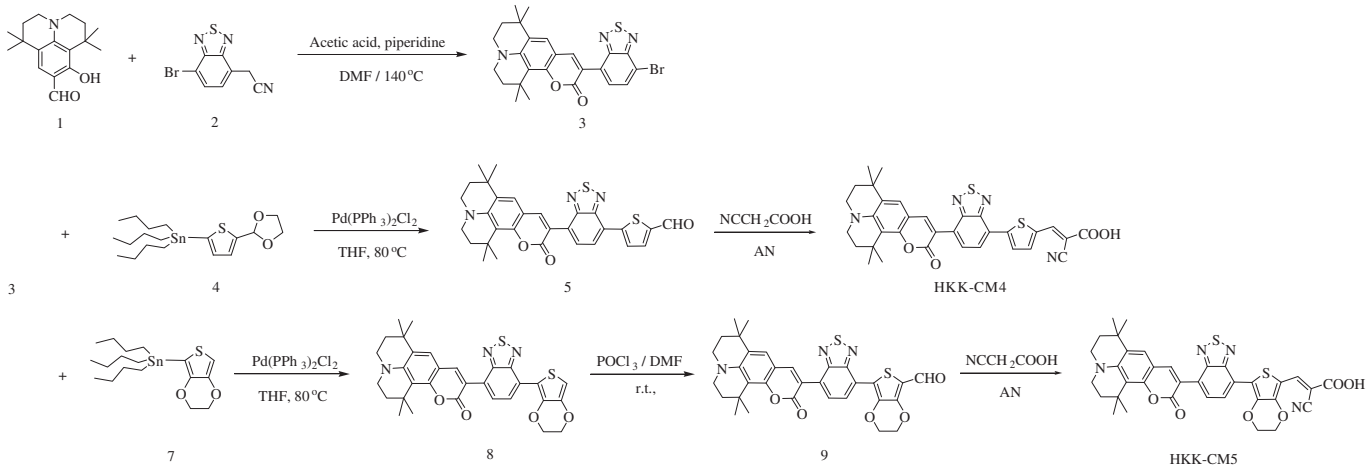

Scheme 1. Chemical structures and synthesis of coumarin dyes containing benzothiadiazole.

connected to a acceptor group in order to destabilise the energy of the highest occupied molecular orbital (HOMO) in D–A–π–A chromophore, leading to a red-shifted absorption and emission band.

2. Experimental

2.1. Materials

All reactions were carried out under a nitrogen atmosphere. Solvents were distilled from appropriate reagents. All reagents were purchased from Aldrich. 9-formyl-1,1,7,7-tetramethyl-2,3,6,7-tetrahydro-1H,5H-pyrido [3,2,1-ij]quinoline [35], 2-(7-bromobenzo [c][1,2,5]thiadiazol-4-yl)acetonitrile [36,37], 2-tri-butylstannyl-3,4-ethyl-enedioxythiophene [38], and 2-tributylstanyl-5-dioxolanylthiophene [39] were synthesised following the same procedures as described previously.

2.2. Measurements

^{1}H NMR spectra were recorded at room temperature with Varian Oxford 300 spectrometers and chemical shifts were reported in ppm units with tetramethylsilane as the internal standard. FT-IR spectra were measured as KBr pellets on a Perkin Elmer Spectrometer. UV–visible absorption spectra were obtained in THF on a Shimadzu UV-2401PC spectrophotometer. Cyclic voltammetry was carried out with a Versa STAT3 (AMETEK). A three-electrode system was used and consisted of a reference electrode (Ag/AgCl), a working electrode, and a platinum wire electrode. The redox potential of dyes on TiO_2 was measured in CH_3CN with 0.1 M $TBAPF_6$ with a scan rate between 50 mV s^{-1}.

2.3. Density functional theory (DFT)/time-dependent DFT (TDDFT) calculations

To better understand the molecular structures of **HKK-CM4** and **HKK-CM5**, we carried out density functional theory (DFT) calculations using the CAM-B3LYP hybrid functional with the 6-311+G** basis set using a suite of Gaussian 09 programs [40]. The protonated **HKK-CM4** and **HKK-CM5** were adapted in DFT calculations. To obtain the photophysical properties of **HKK-CM4** and **HKK-CM5** in THF solution, time-dependent DFT (TDDFT) calculations employing the conductor-like polarisable continuum model (CPCM) [41–44] were performed using the optimised geometries in the gas phase.

2.4. Synthesis

2.4.1. Preparation of 9-(4-bromo-2,1,3-benzothiadiazole-7-yl)-1,1,6,6-tetramethyl-2,3,5,6-tetrahydro-1H,4H,11-oxa-3a-azabenzo [de]anthracen-10-one] (3)

Compound 1 (3.20 g, 11.7 mmol) and compound 2 (3.00 g, 11.8 mmol) were dissolved in 50.0 mL of *N*,*N*-dimethylformamide (DMF), then acetic acid (2.38 mL) and piperidine (4.06 mL) were added to the solution, which was then kept at 140 °C for 6 h. Addition of methanol afforded crystals of compound 3. Yield was 42%. mp 232 °C. ^{1}H NMR ($CDCl_3$) δ (TMS, ppm): 1.32 (6H,s), 1.75 (6H, s), 1.77–1.85 (4H, m), 3.24–3.36 (4H, m), 7.22 (1H, s), 7.89 (1H, d), 8.16 (1H, d), 8.51 (1H, s); ^{13}C NMR (75 MHz, $CDCl_3$) δ 29.13, 30.77, 32.38, 35.87, 39.46, 47.10, 47.56, 109.49, 112.59, 113.82, 114.87, 124.37, 127.93, 128.64, 129.99, 132.52, 145.42, 146.13, 152.67, 153.42, 153.91, 160.82.

2.4.2. Preparation of 5′-(1,1,6,6-tetramethyl-10-oxo-2,3,5,6-tetrahydro-1H,4H,10H,11-oxa-3a-aza-benzo[de]anthracen-9-yl)-[2,1,3-benzothiadiazole]-4-thenyl-5-carbaldehyde (5)

A mixture of compound 3 (0.20 g, 0.39 mmol), compound 4 (0.20 g, 0.45 mmol) and $Pd(PPh_3)_2Cl_2$ (0.02 g, 0.03 mmol) was heated in 50.0 mL of dry THF at 80 °C for 20 h under an inert N_2

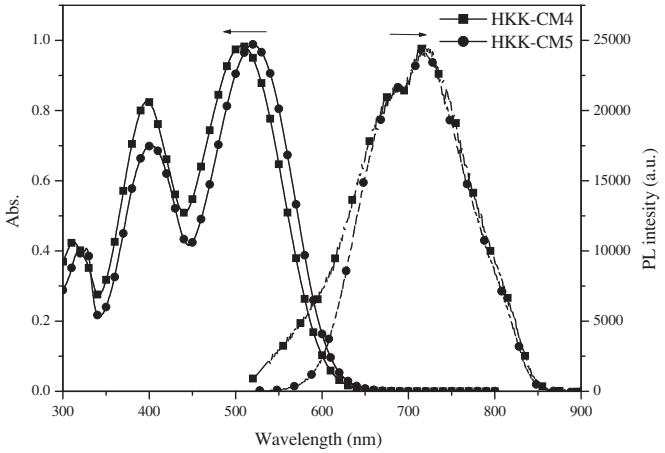

Fig. 1. Absorption and emission spectra of 2×10^{-5} M HKK-CM dyes in $CHCl_3$/MeOH.

Table 1
Optical properties and DSSC performance parameters of HKK-CM dyes.

Dye	Absorption		Emission (λ_{max}/nm)	E_{ox}[b]/V (vs. NHE)	E_{0-0}[c]/V	E_{LUMO}[d]/V (vs. NHE)
	λ_{ma}/(nm),[a] ε (M^{-1} cm^{-1})	λ_{max}/TiO_2 (nm)				
HKK-CM4	397(23,900), 507 (31,000)	336, 494	720	1.06	2.12	−1.06
HKK-CM5	401(23,100), 520 (31,000)	399, 512	720	1.03	2.05	−1.02

[a] Absorption and emission spectra were measured in $CHCl_3$/MeOH.
[b] Oxidation potentials of dyes on TiO_2 were measured in CH_3CN with 0.1 M $TBAPF_6$ with a scan rate of 50 mV s^{-1} (vs. NHE).
[c] E_{0-0} was determined from the intersection of absorption and emission spectra in $CHCl_3$/MeOH.
[d] LUMO was calculated by $E_{ox} - E_{0-0}$.

atmosphere. After concentration, the residue was dissolved in CH_2Cl_2. The organic phase was washed twice with a saturated solution of $NaHCO_3$ and then with water. After drying over $MgSO_4$ and evaporating the solvent, the product was purified by chromatography on silica gel (CH_2Cl_2—hexane 2:1) to give compound 5. Yield was 57%. ^{1}H NMR ($CDCl_3$) δ (TMS, ppm): 1.33 (6H, s), 1.76 (6H, s), 1.78—1.86 (4H, m), 3.25—3.37 (4H, m), 7.25 (1H, s), 7.84 (1H, d), 8.06 (1H, d), 8.17 (1H, d), 8.40 (1H, d), 8.64 (1H, s), 9.98 (1H, s).

*2.4.3. Preparation of 2-cyano-3-[5′-(1,1,6,6-tetramethyl-10-oxo-2,3,5,6-tetrahydro-1H,4H,10H-11-oxa-3a-aza-benzo[de]anthracen-9-yl)-[2,1,3-benzothiadiazole]-4-thiophen-2-yl]-acrylic acid (**HKK-CM4**)*

Compound 5 (0.10 g, 0.18 mmol), dissolved in $CHCl_3$ (20 mL) and acetonitrile (20 mL), was condensed with 2-cyanoacetic acid (0.02 g, 0.29 mmol) in the presence of piperidine (0.03 mL, 0.35 mmol). The mixture was refluxed for 12 h. After cooling the solution, the organic layer was removed *in vacuo*. Dark red solid of **HKK-CM4** was obtained by silica gel chromatography (MC/MeOH = 4:1) Yield was 80%. mp 261 °C. ^{1}H NMR (DMSO-d_6) δ (TMS, ppm): 1.15 (6H, s), 1.51 (6H, s), 1.69—1.98 (4H, m), 3.28—3.32 (4H, m), 7.43 (1H, s), 7.79 (1H, d), 8.11 (1H,s), 8.18—8.21 (3H, m), 8.58 (1H, s); ^{13}C NMR (75 MHz, DMSO-d_6) δ 28.63, 31.71, 31.91, 108.59, 110.858, 112.951, 113.47, 119.37, 124.21, 127.64, 128.26, 138.56, 142.70, 145.90, 151.50, 151.97, 153.14, 159.62, 162.55. UV—vis (THF, nm): λ_{max} (log ε) 397 (23,900), 507 (31,000). PL (THF, nm): λ_{max} 720. FAB-mass: Calcd. for $C_{33}H_{28}N_4O_4S_2$, 608.73; found, 608.00.

2.4.4. Preparation of 9-(4-(3,4-ethylene dioxythiophene)-2,1,3-benzothiadiazole-7-yl)-1,1,6,6-tetramethyl-2,3,5,6-tetrahydro-1H,4H,11-oxa-3a-azabenzo[de]anthracen-10-one] (7)

A mixture of compound 3 (0.20 g, 0.39 mmol), compound 6 (0.25 g, 0.58 mmol) and $Pd(PPh_3)_2Cl_2$ (0.02 g, 0.03 mmol) was heated in 50.0 mL of dry THF at 80 °C for 20 h under an inert N_2 atmosphere. After concentration, the residue was dissolved in CH_2Cl_2. The organic phase was washed twice with a saturated solution of $NaHCO_3$ and then with water. After drying over $MgSO_4$ and evaporating the solvent, the product was purified by silica gel chromatography (MC/Hex = 2:1) to give compound 7. Yield was 62%. ^{1}H NMR ($CDCl_3$) δ (TMS, ppm): 1.33 (6H, s), 1.75 (6H, s), 1.77—1.86 (4H, m), 3.23—3.35 (4H, m), 4.31—4.44 (4H, m), 6.58 (1H, s), 7.24 (1H, d), 8.31 (1H, d), 8.41 (1H, d), 8.55 (1H, s).

2.4.5. Preparation of 5′-(1,1,6,6-tetramethyl-10-oxo-2,3,5,6-tetrahydro-1H,4H,10H,11-oxa-3a-aza-benzo[de]anthracen-9-yl)-[2,1,3-thiadiazole]-4-(3,4-ethylene dioxythiophenyl)-5-carbaldehyde (8)

$POCl_3$ (0.03 mL, 0.34 mmol) was slowly added to 15 mL of anhydrous DMF under a nitrogen atmosphere at 0 °C. The mixture was vigorously stirred for 2 h, then compound 7 was dissolved in 10 mL of anhydrous DMF. After 12 h at room temperature, the solution was added dropwise on ice, then NaOAc(aq) was added until a pH of 7—8 was achieved. The mixture was extracted with dichloromethane and brine. After drying over $MgSO_4$ and evaporating the solvent, the product was purified by silica gel chromatography (MC/Hex = 2:1) to give compound 8. Yield was 59%. ^{1}H NMR ($CDCl_3$) δ (TMS, ppm): 1.34 (6H,s), 1.62 (6H, s), 1.79—1.87 (4H, m), 3.26—3.38 (4H, m), 4.50 (4H, s), 7.27 (1H, s), 8.42 (1H, d), 8.55 (1H, d), 8.68 (1H, s), 10.0 (1H, s).

*2.4.6. Preparation of 2-cyano-3-[5′-(1,1,6,6-tetramethyl-10-oxo-2,3,5,6-tetrahydro-1H,4H,10H-11-oxa-3a-aza-benzo[de]anthracen-9-yl)-[2,1,3-benzothiadiazole]-4-(3,4-ethylene dioxythiopheneyl-5-yl)]-acrylic acid (**HKK-CM5**)*

Compound 8 (0.08 g, 0.13 mmol), dissolved in $CHCl_3$ (20 mL) and acetonitrile (20 mL), was condensed with 2-cyanoacetic acid (0.02 g, 0.21 mmol) in the presence of piperidine (0.03 mL, 0.35 mmol). The mixture was refluxed for 12 h. After cooling the solution, the organic layer was removed *in vacuo*. Dark red solid of **HKK-CM5** was obtained by silica gel chromatography (MC/MeOH = 3:1) Yield was 75%. mp 276 °C. ^{1}H NMR (DMSO-d_6) δ (TMS, ppm): 1.28 (6H, s), 1.52 (6H, s), 1.72—1.80 (4H, m), 3.28—3.32 (4H, m), 4.49—3.32 (4H, m), 7.44 (1H, s), 8.09 (1H, s), 8.19 (1H, d), 8.47 (1H, d), 8.59 (1H, s); ^{13}C NMR (75 MHz, DMSO-d_6) δ 28.62, 29310, 30.38, 31.70, 31.89, 56.44, 64.83, 107.91, 108.61, 113.08, 113.50, 113.91, 116.43, 119.77, 123.34, 126.63, 128.24, 129.23, 140.28, 144.17, 145.83, 151.49, 151.93, 152.96, 159.62, 162.75. UV—vis (THF, nm): λ_{max} (log ε) 401 (25,100), 520 (31,000). PL (THF, nm): λ_{max} 720. FAB-mass: calcd. for $C_{35}H_{30}N_4O_6S_2$, 666.77; found, 667.00.

2.5. Fabrication and testing of DSSC

FTO glass plates (Pilkington) were cleaned in a detergent solution using an ultrasonic bath for 1 h, then rinsed with water and ethanol. The FTO glass plates were immersed in an aqueous solution of 40 mM $TiCl_4$ at 70 °C for 30 min and then washed with water and ethanol. The first TiO_2 layer with a thickness of 8 μm was prepared by screen-printing TiO_2 paste (Solaronix, 13 nm anatase), and the

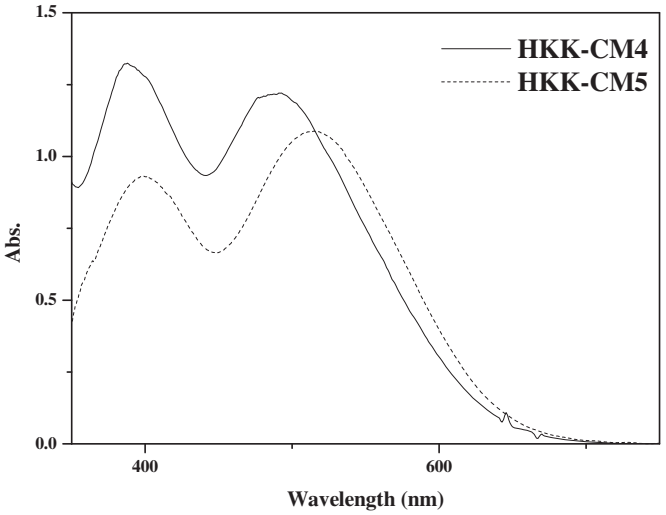

Fig. 2. Absorption spectra of HKK-CM dyes on 2 μm TiO_2 transparent films.

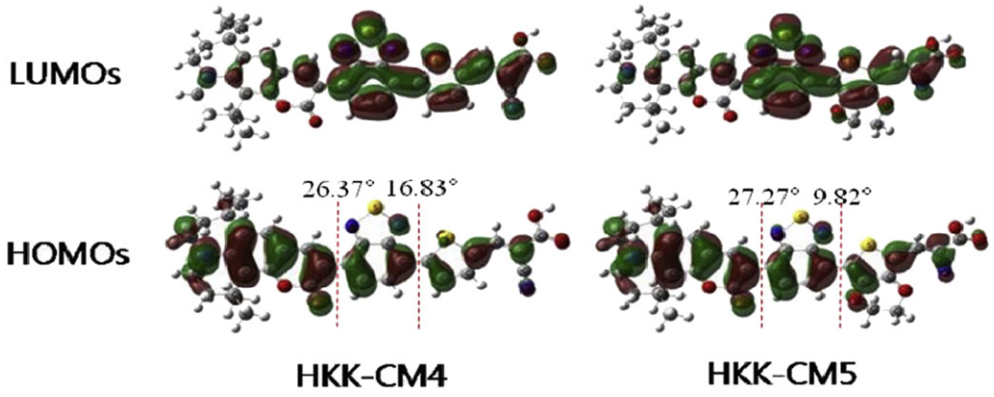

Fig. 3. Plots of the isodensity surfaces (B3LYP/6-31G* in THF) of the HOMOs and LUMOs of HKK-CM dyes.

second scattering layer containing 400 nm sized anatase particles was deposited by screen-printing. The TiO_2 electrodes were immersed into the dye solution (0.3 mM) in $CHCl_3$/MeOH (3:1) with DCA (40 mM) and kept at room temperature overnight. Counter electrodes were prepared by coating with a drop of H_2PtCl_6 solution (2 mg of Pt in 1 mL of ethanol) on an FTO plate. The dye-adsorbed TiO_2 electrode and Pt counter electrode were assembled in a sealed sandwich-type cell. One drop of electrolyte was then introduced into the cell, which was composed of 0.6 M 1,2-dimetyl-3-propyl imidazolium iodide, 0.05 M iodine, 0.1 M LiI, and 0.5 M *tert*-butylpyridine in acetonitrile. The electrolyte was introduced into the inter-electrode space from the counter electrode side through pre-drilled holes. The drilled holes were sealed with a microscope cover slide and Surlyn to avoid leakage of the electrolyte solution.

2.6. Photoelectrochemical measurements of DSSC

Photoelectrochemical data were measured using a 1000 W xenon light source (Oriel, 91193) that was focused to give 1000 W/m^2, the equivalent of one sun at AM 1.5G, at the surface of the test cell. The light intensity was adjusted with a Si solar cell that was double-checked with an NREL-calibrated Si solar cell (PV Measurement Inc.). The applied potential and measured cell current were measured using a Keithley model 2400 digital source meter. The current–voltage characteristics of the cell under these conditions were determined by biasing the cell externally and measuring the generated photocurrent. This process was fully automated using Wavemetrics software.

3. Results and discussion

The synthetic procedures of coumarin dyes containing benzothiadiazole are depicted in Scheme 1. Coumarin aldehyde derivatives were synthesised by either a Vilsmeier–Haack or Stille coupling reaction. These aldehydes, upon reaction with cyanoacetic acid in the presence of a piperidine catalyst, produced the coumarin dyes presented here.

Fig. 1 shows the absorption and emission spectra of coumarin dyes measured in $CHCl_3$/MeOH solution; their photophysical properties are summarised in Table 1. The absorption spectrum of the **HKK-CM5** dye, with the introduction of an EDOT unit into the thiophene-containing coumarin dye **HKK-CM4** to up-lift the HOMO level and down-shift the LUMO, showed a maximum absorption of 520 nm ($\varepsilon = 31{,}000\ M^{-1}\ cm^{-1}$), which was 13 nm red-shifted in contrast to **HKK-CM4**. The absorption spectra of **HKK-CM** dyes on the surface of TiO_2 are shown in Fig. 2. Typically, the blue shift on TiO_2 is a common phenomenon for most organic dyes, which is regarded as the result of a strong interaction between the dye and the semiconductor surface. A similar trend has been demonstrated when dyes were deprotonated in the presence of a base. However, such an effect is partially annihilated by the D–A–π–A system. [34]

The electrochemical properties were investigated by cyclic voltammetry (CV) to obtain the HOMO and LUMO levels of the present dyes. The cyclic voltammogram curves were obtained from a three-electrode cell in 0.1 M $TBAPF_6$ in CH_3CN at a scan rate of 50 mV/s, using a dye-coated TiO_2 electrode as the working electrode, a Pt wire counter-electrode, and an Ag/AgCl (saturated KCl) reference electrode (+0.197 V vs. NHE) which was calibrated with ferrocene. All of the measured potentials were converted to the NHE scale. The band-gap was estimated from the absorption edges of UV–vis spectra and LUMO energy levels were derived from the HOMO energy levels and the band-gap. HOMO values (1.03–1.06 V vs. NHE) were more positive than the I^-/I_3^- redox couple (0.4 V vs. NHE). Electron injection from the excited sensitisers to the conduction band of TiO_2 should be energetically favourable because of the more negative LUMO values (−1.02 to −1.06 vs. NHE) compared to the conduction band edge energy level of the TiO_2 electrode [45]. The shapes of HOMO and LUMO of **HKK-CM4** and **HKK-CM5** are shown in Fig. 3. The dihedral angles between the benzothiadiazole moiety and the coumarin moiety in **HKK-CM4** and **HKK-CM5** were calculated to be 26.37° and 27.27°, respectively. On the other hand, the dihedral angle between the thiophene/EDOT

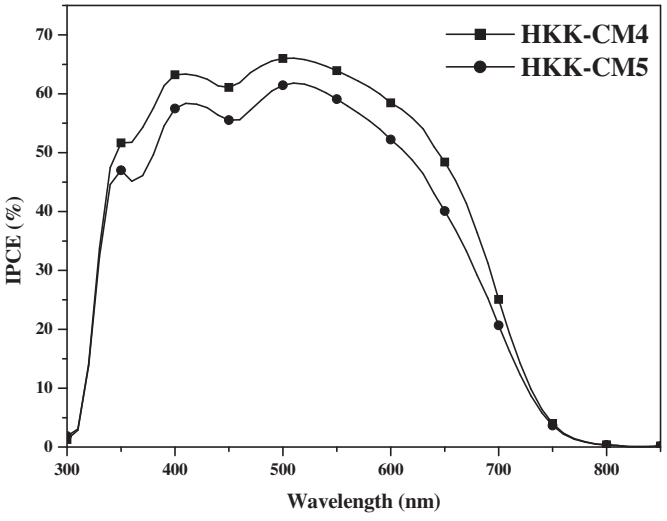

Fig. 4. Typical action spectra of incident photon-to-current conversion efficiencies (IPCE) obtained for nanocrystalline TiO_2 solar cells sensitized by HKK-CM dyes.

Table 2
Dye-sensitised solar cell performance data of the HKK-CM dyes.

Dye	DCA (mM)	$\Gamma/10^{-7}$ (mol cm^{-2})	J_{SC} (mA/cm^2)	V_{OC} (V)	FF	η (%)
HKK-CM4	0	2.3	12.2	0.58	0.68	4.82
	40	1.3	14.3	0.58	0.72	5.97
HKK-CM5	0	2.2	10.8	0.55	0.66	3.93
	40	1.7	13.3	0.56	0.68	5.03
N719	–	–	16.7	0.71	0.73	8.64

TiO_2 thickness 9,5+4,sc,$TiCl_4$; electrolyte condition 0.6 M DMPII, 0.5 M LiI, 0.05 M I_2, 0.5 M TBP in an acetonitrile solution; dye was dissolved in $CHCl_3$/MeOH.

moiety and the benzothiadiazole moiety in **HKK-CM4** and **HKK-CM5** were calculated to be 16.83° and 9.82°, respectively. The structural difference was negligible for the dihedral angle between the benzothiadiazole and coumarin moieties; however, the thiophene of **HKK-CM4** and the EDOT of **HKK-CM5** caused a remarkable difference in the dihedral angle with benzothiadiazole; **HKK-CM4** possessed a more tilted structure than **HKK-CM5**. As shown in Fig. 3, the shapes of HOMO and LUMO for both compounds were very similar. The electrons of HOMO in both compounds were distributed over the entire conjugated chromophore, while those of LUMO were mainly distributed over the benzothiadiazole-substituted thiophene (or EDOT) moiety. It was found that HOMO-1 → LUMO, HOMO → LUMO, and HOMO → LUMO + 1 contributed to the lowest transitions of **HKK-CM4** and **HKK-CM5**. The calculated excitation energies of **HKK-CM4** and **HKK-CM5** in THF were calculated to be 2.5822 and 2.5713 eV, respectively, which correspond to absorption wavelengths of 480.16 and 482.18 nm, respectively. The red-shifted absorption of **HKK-CM5** as compared with **HKK-CM4** could be explained in terms of the effective conjugation. **HKK-CM5** showed better planarity, hence better conjugation than **HKK-CM4**, thus charge-transfer excitation in **HKK-CM5** was easier than in **HKK-CM4**.

Fig. 4 shows the incident monochromatic photon-to-current conversion efficiency (IPCE) of the sensitised coumarin dyes. The onset wavelengths of the IPCE spectra for DSSCs based on **HKK-CM4** and **HKK-CM5** were 800 nm. IPCE values higher than 60% were observed in the range of 410–605 nm with a maximum value of 66% at 500 nm for the DSSC based on **HKK-CM4**. The maximum IPCE value of the DSSC based on **HKK-CM5** was slightly lower than the efficiencies of the DSSC based on **HKK-CM4** due to the increased intermolecular π–π interaction with introduction of EDOT.

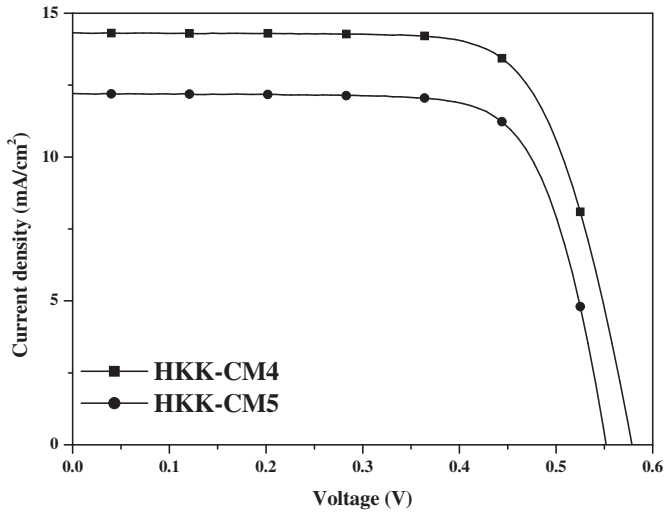

Fig. 5. Photocurrent–voltage characteristics of representative TiO_2 electrodes sensitized with HKK-CM dyes.

The photovoltaic performance of the coumarin DSSC are summarised in Table 2. Under the standard global AM 1.5 solar condition, the **HKK-CM4** sensitised cell gave a short circuit photocurrent density (J_{SC}) of 14.3 mA cm^{-2}, an open circuit voltage (V_{OC}) of 0.58 V, and a fill factor (FF) of 0.72 (Fig. 5), corresponding to an overall conversion efficiency η 5.97%. The **HKK-CM5** sensitised cell gave a J_{SC} of 13.3 mA cm^{-2}, a V_{OC} of 0.56 V, and an FF of 0.68, corresponding to an overall conversion efficiency η of 5.03%. We observed that the adsorbed dye amount of **HKK-CM5** dye larger than adsorbed dye amount of **HKK-CM4** dye with DCA as a co-adsorbent. This can be rationalized by the increased intermolecular π–π interaction with introduction of EDOT. The EDOT unit in **HKK-CM5** may lead to strong π–π interaction which would decrease the lower efficiency of electron injection [46].

4. Conclusions

Coumarin dyes containing low band-gap chromophores were designed and synthesised. The D–A–π–A system of the dyes could effectively elongate the absorption wavelength. A wider wavelength of absorption was favourable for the light-harvesting efficiency of DSSCs. The **HKK-CM5** dye had a broader light harvesting range than **HKK-CM4**, while strong π–π interaction in **HKK-CM5** was less efficient than that of **HKK-CM4**, due to the introduction of EDOT moiety. As a result, the solar cell based on the **HKK-CM4** sensitiser showed better photovoltaic performance than **HKK-CM5**-based solar cells, with a J_{SC} of 14.3 mA cm^{-2}, a V_{OC} of 0.58 V, and an FF of 0.72, corresponding to an overall conversion efficiency η of 5.97% under standard AM 1.5 irradiation.

Acknowledgements

This research was supported by the New & Renewable Energy of the Korea Institute of Energy Technology Evaluation and Planning (KETEP) grant funded by the Korea Government Ministry of Knowledge Economy (gs1) (no. 20103060010020), the WCU (the Ministry of Education and Science (gs2)) programme (R31-2008-000-10035-0) and the Converging Research Centre programme through the Ministry of Education, Science and Technology (gs3) (2010K000973). The work at SKKU was supported by an NRF grant (2011-0001211) funded by MEST (gs4).

Appendix. Supplementary material

Supplementary material associated with this article can be found, in the online version, at doi:10.1016/j.dyepig.2012.02.015.

References

[1] Nazeeruddin MK, De Angelis F, Fantacci S, Selloni A, Viscardi G, Grätzel M, et al. Combined experimental and DFT-TDDFT computational study of photoelectrochemical cell ruthenium sensitizers. J Am Chem Soc 2005;127:16,835–16,847.
[2] Nazeeruddin MK, Pechy P, Renouard T, Zakeeruddin SM, Humphry-Baker R, Grätzel M, et al. Engineering of efficient panchromatic sensitizers for nanocrystalline TiO_2-based solar cells. J Am Chem Soc 2001;123:1613–24.
[3] Mishra A, Fischer MKR, Bäuerle P. Metal-free organic dyes for dye-sensitized solar cells: from structure: property relationships to design rules. Angew Chem Int Ed 2009;48:2474–99.
[4] Ning Z, Fu Y, Tian H. Improvement of dye-sensitized solar cells: what we know and what we need to know. Energy Environ Sci 2010;3:1170–81.
[5] Asbury JB, Ellingson RJ, Gosh HN, Ferrere S, Notzig AJ, Lian T. Femtosecond IR study of excited-state relaxation and electron-injection dynamics of Ru(dcbpy)$_2$(NCS)$_2$ in solution and on nanocrystalline TiO_2 and Al_2O_3 thin films. J Phys Chem B 1999;103:3110–9.
[6] Park NG, Kang MG, Kim KM, Ryu KS, Kim DK, Frank AJ, et al. Morphological and photoelectrochemical characterization of core-shell nanoparticle films for dye-sensitized solar cells: Zn–O type shell on SnO_2 and TiO_2 cores. Langmuir 2004;20:4246–53.

[7] Saito Y, Fukuri N, Senadeera R, Kitamura T, Wada Y, Yanagida S. Solid state dye sensitized solar cells using in situ polymerized PEDOTs as hole conductor. Electrochem Commun 2004;6:71–4.
[8] Fabregat-Santiago F, Garcia-Cañadas J, Palomares E, Clifford JN, Durrant JR, Bisquert J, et al. The origin of slow electron recombination processes in dye-sensitized solar cells with alumina barrier coatings. J Appl Phys 2004;96:6903–7.
[9] Furube A, Katoh R, Hara K, Murata S, Arakawa H, Tachiya M, et al. Ultrafast direct and indirect electron-injection processes in a photoexcited dye-sensitized nanocrystalline zinc oxide film: The importance of exciplex intermediates at the surface. J Phys Chem B 2004;108:12583–92.
[10] Tian H, Meng F. Organic photovoltaics: mechanisms, materials, and devices. London: CRC; 2005.
[11] Seo KD, Song HM, Lee MJ, Nazeeruddin MK, Gräetzel M, Kim HK, et al. Coumarin dyes containing low-band-gap chromophores for dye-sensitised solar cells. Dyes Pigments 2011;90:304–10.
[12] Hara K, Wang ZS, Sato T, Furube A, Katoh R, Sugihara H, et al. Oligothiophene-containing coumarin dyes for efficient dye-sensitized solar cells. J Phys Chem B 2005;109:15476–82.
[13] Ning Z, Tian H. Triarylamine: a promising core unit for efficient photovoltaic materials. Chem Commun; 2009:5483–95.
[14] Lee DH, Lee MJ, Song HM, Song BJ, Seo KD, Kim HK, et al. Organic dyes incorporating low-band-gap chromophores based on p-extended benzothiadiazole for dye-sensitized solar cells. Dyes Pigments 2011;91:192–8.
[15] Ning Z, Zhang Q, Wu W, Pei H, Liu B, Tian H. Starburst triarylamine based dyes for efficient dye-sensitized solar cells. J Org Chem 2008;73:3791–7.
[16] Li G, Jiang KJ, Li YF, Li SL, Yang LM. Efficient structural modification of triphenylamine-based organic dyes for dye-sensitized solar cells. J Phys Chem C 2008;112:11591–9.
[17] Wang ZS, Li FY, Huang CH, Wang L, Wei M, Jin LP, et al. Photoelectric conversion properties of nanocrystalline TiO_2 electrodes sensitized with hemicyanine derivatives. J Phys Chem B 2000;104:9676–82.
[18] Chen YS, Li C, Zeng ZH, Wang WB, Wang XS, Zhang BW. Efficient electron injection due to a special adsorbing group's combination of carboxyl and hydroxyl: dye-sensitized solar cells based on new hemicyanine dyes. J Mater Chem 2005;15:1654–61.
[19] Tanaka K, Takimiya K, Otsubo T, Kawabuchi K, Kajihara S, Harima Y. Development and photovoltaic performance of oligothiophene-sensitized TiO_2 solar cells. Chem Lett 2006;35:592–3.
[20] Horiuchi T, Miura H, Uchida S. Highly efficient metal-free organic dyes for dye-sensitized solar cells. J Photochem Photobiol A Chem 2004;164:29–32.
[21] Horiuchi T, Miura H, Sumioka K, Uchida S. High efficiency of dye-sensitized solar cells based on metal-free indoline dyes. J Am Chem Soc 2004;126:12218–9.
[22] Schmidt-Mende L, Bach U, Humphry-Baker R, Horiuchi T, Miura H, Ito S, et al. Organic dye for highly efficient solid-state dye-sensitized solar cells. Adv Mater 2005;17:813–5.
[23] Ito S, Zakeeruddin SM, Humphry-Baker R, Liska P, Charvët R, Grätzel M, et al. High-efficiency organic-dye-sensitized solar cells controlled by nanocrystalline-TiO_2 electrode thickness. Adv Mater 2006;18:1202–5.
[24] Howie WH, Claeyssens F, Miura H, Peter ML. Characterization of solid-state dye-sensitized solar cells utilizing high absorption coefficient metal-free organic dyes. J Am Chem Soc 2008;130:1367–75.
[25] Kuang D, Uchida S, Humphry-Baker R, Zakeeruddin SK, Grätzel M. Organic dye-sensitized ionic liquid based solar cells: remarkable enhancement in performance through molecular design of indoline sensitizers. Angew Chem Int Ed 2008;47:1923–7.
[26] Ito S, Miura H, Uchida S, Takata M, Sumioka K, Liska P, et al. High-conversion-efficiency organic dye-sensitized solar cells with a novel indoline dye. Chem Commun; 2008:5194–6.
[27] Kang MS, Oh JB, Seo KD, Roh SG, Kim HK, Kim K, et al. Novel extended p-conjugated Zn(II)-porphyrin derivatives bearing pendant triphenylamine moiety for dye-sensitized solar cell: synthesis and characterization. J Porphyrins Phthalocyanines 2009;13:798–804.
[28] Imahori H, Umeyama T, Ito S. Large π-aromatic molecules as potential sensitizers for highly efficient dye-sensitized solar cells. Acc Chem Res 2009;42:1809–18.
[29] Lee MJ, Seo KD, Song HM, Kang HS, Kim HK, et al. Novel D–π–A system based on zinc-porphyrin derivatives for highly efficient dye-sensitised solar cells. Tetrahedron Lett 2011;52:3879–82.
[30] Imahori H, Matsubara Y, Iijima H, Umeyama T, Matano Y, Ito S, et al. Effects of *meso*-diarylamino group of porphyrins as sensitizers in dye-sensitized solar cells on optical, electrochemical, and photovoltaic properties. J Phys Chem C 2010;114:10656–65.
[31] Mai CL, Huang WK, Lu HP, Lee CW, Diau EWG, Yeh CY, et al. Synthesis and characterization of diporphyrin sensitizers for dye-sensitized solar cells. Chem Commun 2010;46:809–11.
[32] Eu S, Katoh T, Umeyama T, Matano Y, Imahori H. Synthesis of sterically hindered phthalocyanines and their applications to dye-sensitized solar cells. Dalton Trans; 2008:5476–83.
[33] Wang ZS, Cui Y, Hara K, Dan-Oh Y, Kasada C, Shinpo A. A high-light-harvesting-efficiency coumarin dye for stable dye-sensitized solar cells. Adv Mater 2007;19:1138–41.
[34] Zhu W, Wu Y, Wang S, Li W, Wang Z, Tian H. Organic D–A–π–A solar cell sensitizers with improved stability and spectral response. Adv Funct Mater 2010;21:756–63.
[35] Lee CC, Hu AT. Synthesis and optical recording properties of some novel styryl dyes for DVD-R. Dyes Pigments 2003;59:63–9.
[36] Jørgensen M, Krebs FC. Stepwise unidirectional synthesis of oligo phenylene vinylenes with a series of monomers. Use in plastic solar cells. J Org Chem 2005;70:6004–17.
[37] Sundaresan AK, Ramamurthy V. Making a difference on excited-state chemistry by controlling free space within a nanocapsule: Photochemistry of 1-(4-alkylphenyl)-3-phenylpropan-2-ones. Org Lett 2007;9:3575–8.
[38] Hauck SI, Lakshmi KV, Hartwig JF. Tetraazacyclophanes by palladium-catalyzed aromatic amination. Geometrically defined, stable, high-spin diradicals. Org Lett 1999;1:2057–60.
[39] Hergué N, Leriche P, Blanchard P, Allain M, Gallego-Planas N, Frére P, et al. Evidence for the contribution of sulfur–bromine intramolecular interactions to the self-rigidification of thiophene-based π-conjugated systems. New J Chem 2008;32:932–6.
[40] Frisch MJ, Trucks GW, Schlegel HB, Scuseria GE, Robb MA, Cheeseman JR, et al. Gaussian 09. Wallingford CT: Gaussian, Inc; 2009.
[41] Klamt A, Schüürmann G. COSMO: a new approach to dielectric screening in solvents with explicit expressions for the screening energy and its gradient. J Chem Soc, Perkin Trans 1993;2:799–805.
[42] Andzelm J, Kölmel C, Klamt A. Incorporation of solvent effects into density functional calculations of molecular energies and geometries. J Chem Phys 1995;103:9312–20.
[43] Barone V, Cossi M. Quantum calculation of molecular energies and energy gradients in solution by a conductor solvent model. J Phys Chem A 1998;102:1995–2001.
[44] Cossi M, Rega N, Scalmani G, Barone V. Energies, structures, and electronic properties of molecules in solution with the C-PCM solvation model. J Comput Chem 2003;24:669–81.
[45] Hagfeldt A, Grätzel M. Light-induced redox reactions in nanocrystalline systems. Chem Rev 1995;95:49–68.
[46] Wang ZS, Koumura N, Cui Y, Takahashi M, Sekiguchi H, Hara K, et al. Hexylthiophene-functionalized carbazole dyes for efficient molecular photovoltaics: tuning of solar-cell performance by structural modification. Chem Mater 2008;20:3993–4003.